

RESEARCH ARTICLE

NADH dehydrogenases drive inward electron transfer in *Shewanella oneidensis* MR-1

Nicholas M. Tefft¹ | Kathryn Ford^{1,2} | Michaela A. TerAvest¹ 

¹Department of Biochemistry and Molecular Biology, Michigan State University, East Lansing, Michigan, USA

²Department of Microbiology and Molecular Genetics, Michigan State University, East Lansing, Michigan, USA

Correspondence

Michaela A. TerAvest, Department of Biochemistry and Molecular Biology, Michigan State University, East Lansing, MI, USA.

Email: teraves2@msu.edu

Funding information

National Science Foundation Graduate Research Fellowship, Grant/Award Number: DGE-1848739; National Science Foundation CAREER Award, Grant/Award Number: 1750785; 2018 Beckman Young Investigator Award

Abstract

Shewanella oneidensis MR-1 is a promising chassis organism for microbial electrosynthesis because it has a well-defined biochemical pathway (the Mtr pathway) that can connect extracellular electrodes to respiratory electron carriers inside the cell. We previously found that the Mtr pathway can be used to transfer electrons from a cathode to intracellular electron carriers and drive reduction reactions. In this work, we hypothesized that native NADH dehydrogenases form an essential link between the Mtr pathway and NADH in the cytoplasm. To test this hypothesis, we compared the ability of various mutant strains to accept electrons from a cathode and transfer them to an NADH-dependent reaction in the cytoplasm, reduction of acetoin to 2,3-butanediol. We found that deletion of genes encoding NADH dehydrogenases from the genome blocked electron transfer from a cathode to NADH in the cytoplasm, preventing the conversion of acetoin to 2,3-butanediol. However, electron transfer to fumarate was not blocked by the gene deletions, indicating that NADH dehydrogenase deletion specifically impacted NADH generation and did not cause a general defect in extracellular electron transfer. Proton motive force (PMF) is linked to the function of the NADH dehydrogenases. We added a protonophore to collapse PMF and observed that it blocked inward electron transfer to acetoin but not fumarate. Together these results indicate a link between the Mtr pathway and intracellular NADH. Future work to optimize microbial electrosynthesis in *S. oneidensis* MR-1 should focus on optimizing flux through NADH dehydrogenases.

INTRODUCTION

As sustainable methods of electricity generation have expanded, so has interest in using electrical energy to power the electrochemical reduction of CO₂ into useful products, a process called electrosynthesis. However, electrosynthesis is still in early stages of development and there are currently no catalysts with the efficiency and longevity to make electrosynthesis economically viable (Pappijn et al., 2020). Microbes are an attractive option for catalysing electrosynthesis because they are self-renewing and can be genetically modified to produce molecules with unparalleled specificity. To be a

good catalyst for electrosynthesis, a microbe must be able to accept electrons efficiently from an extracellular electrode and use them to generate intracellular reducing equivalents that can be used to drive metabolic pathways (Rabaey & Rozendal, 2010). Some attempts have been made to isolate an organism from nature with the capability for electrosynthesis, but none of the isolates have proved easy to culture or genetically modify (Eddie et al., 2017; Rowe et al., 2015). Some natural candidates are iron-oxidizing bacteria and acetogens (which fix CO₂ using inorganic electron donors), and some success in electrosynthesis has been demonstrated with both groups of organisms (Bose et al., 2014; Nevin et al., 2011).

This is an open access article under the terms of the [Creative Commons Attribution-NonCommercial](https://creativecommons.org/licenses/by-nc/4.0/) License, which permits use, distribution and reproduction in any medium, provided the original work is properly cited and is not used for commercial purposes.

© 2022 The Authors. *Microbial Biotechnology* published by Applied Microbiology International and John Wiley & Sons Ltd.

Another avenue to microbial electrosynthesis is to focus on organisms that are known as metal reducers and support much higher extracellular electron transfer rates, although in the outward rather than inward direction. Metal-reducing bacteria use solid metal oxides as terminal electron acceptors for respiration in nature and can use electrodes as an electron acceptor in the laboratory (Bond & Lovley, 2003; Hernandez & Newman, 2001; Myers & Neelson, 1988). Model metal reducers, such as *Shewanella oneidensis* and *Geobacter sulfurreducens* have well-understood biochemical pathways that connect intracellular electron carriers with extracellular electrodes (Coursolle & Gralnick, 2010; Levar et al., 2014; Marritt et al., 2012; Richardson et al., 2012; Shi et al., 2012, 2014). In *S. oneidensis*, the reversibility of this pathway has been demonstrated by multiple research groups (Ross et al., 2011; Rowe et al., 2018, 2021). Recently, Rowe et al. (Rowe et al., 2021) have proposed that there may also be a dedicated pathway in *S. oneidensis* MR-1 for electron uptake in natural settings. In all previous studies, electron transfer proceeded from the cathode through the electron transport chain to a native terminal electron acceptor, such as oxygen or fumarate (Figure 1).

To use *S. oneidensis* for microbial electrosynthesis, electrons must be transferred from the cathode to intracellular electron carriers, such as NADH. We previously developed a system in *S. oneidensis* MR-1 to enable electrode-driven reduction of exogenous acetoin to 2,3-butanediol in the cytoplasm, a process that is NADH-dependent. We engineered a strain of *S. oneidensis* carrying butanediol dehydrogenase (Bdh) and proteorhodopsin (PR) on a plasmid with constitutive expression (Figure 1). We observed that the modified *S. oneidensis* catalysed acetoin reduction to 2,3-butanediol and that the reduction was dependent on both an active cathode and PR (Tefft & TerAvest, 2019). These results indicated that electrons from the cathode can be used to generate intracellular NADH.

Here, we hypothesize that native NADH dehydrogenases form the link between quinones (which are reduced directly by CymA) and intracellular NADH and that a source of proton motive force (PMF) is necessary to drive NADH dehydrogenases in reverse. The redox potential for the menaquinone/menaquinol pair ($-80\text{ mV}_{\text{SHE}}$) is more positive than the redox potential for the NADH/NAD⁺ pair ($-320\text{ mV}_{\text{SHE}}$), making the electron transfer thermodynamically unfavourable (Flamholz et al., 2012). Although ubiquinone could theoretically also be used as an electron carrier for inward electron transfer, it would be even more unfavourable to transfer electrons to NAD⁺ because of the more positive redox potential of ubiquinone ($+80\text{ mV}_{\text{SHE}}$). Further, menaquinone is the redox partner of CymA, suggesting that it is likely the main quinone involved in extracellular electron transfer (McMillan et al., 2012). In the ‘forward’ reaction during respiration, electrogenic NADH dehydrogenases catalyse the favourable electron transfer from NADH to quinones and conserve energy by coupling the electron transfer with proton or sodium movement against their gradients, thus forming a proton motive force (PMF) or sodium motive force (SMF). These complexes are also capable of reverse electron transfer in some contexts, coupling the reverse (unfavourable) electron transfer with the favourable movement of protons or sodium ions with the gradient, thus dissipating PMF or SMF (Spero et al., 2015). The *S. oneidensis* MR-1 genome encodes four NADH dehydrogenases, Nuo (SO_1009 to SO_1021), Nqr1 (SO_1103 to SO_1108), Nqr2 (SO_0902 to SO_0907) and Ndh (SO_3517). Nuo couples electron transfer with proton transfer, while Nqr1 and Nqr2 couple electron transfer with sodium ion transfer, and Ndh does not transfer any ions across the membrane.

To test whether NADH dehydrogenases participate in inward electron transfer to acetoin, we measured the ability of strains lacking NADH dehydrogenases to carry out this process. We previously studied the NADH dehydrogenases of *S. oneidensis* under a range of growth conditions and found that only Nuo and Nqr1 have a

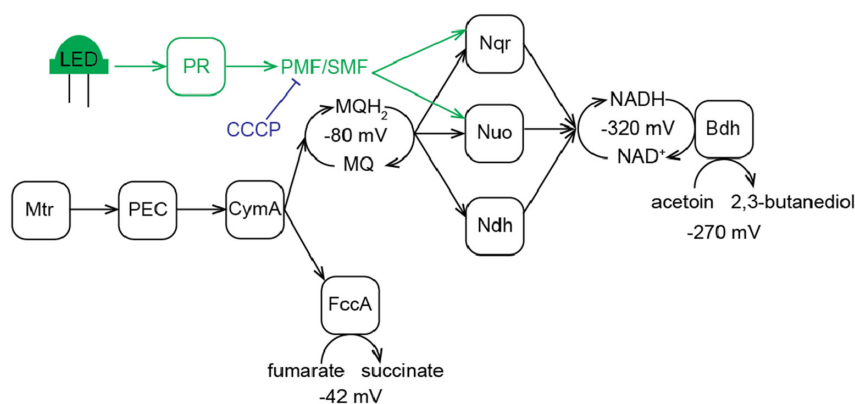


FIGURE 1 *Shewanella oneidensis* MR-1 inward electron transfer pathways. Black arrows indicate electron transfer steps. CCCP, Cyanide m-chlorophenyl hydrazine; LED, Green light light-emitting diode; MQ, Menaquinone; MQH₂, Menaquinol; PEC, Periplasmic electron carriers (e.g., FccA, CctA); PMF, Proton motive force; PR, Proteorhodopsin; SMF, sodium motive force.

significant impact on growth (Duhl et al., 2018; Duhl & Ter Avest, 2019; Madsen & TerAvest, 2019). Therefore, we focused only on those two complexes in this work. Further, we evaluated the role of PMF in this system by testing the effect of the protonophore cyanide m-chlorophenyl hydrazone (CCCP) on inward electron transfer.

EXPERIMENTAL PROCEDURES

Strains, plasmids and growth conditions

Strains and plasmids used in this study are listed in Table 1 and grown as previously described (Duhl et al., 2018) with the following modifications. M5T medium was additionally supplemented with 0.1% tryptone. M5 medium with the following modifications was used in the working electrode chamber during bioelectrochemical experiments: 100mM HEPES, no carbon source, no casamino acids. Working chambers were further supplemented with 0.2 μ M riboflavin prior to inoculation. For aerobic 2,3-butanediol experiments, 50ml of LB supplemented with 50 μ g/ml kanamycin and 10mM acetoin were inoculated with 100 μ l of bacterial culture standardized to OD = 1 then grown at 30°C shaking in a 250ml flask. Samples were taken at 18, 22 and 46h.

Deletion of hydrogenase genes and transformation of BDH-PR plasmid

Hydrogenase knockout mutants were prepared in existing NADH dehydrogenase backgrounds, (Duhl

et al., 2018) using pSMV3.0 (Saltikov & Newman, 2003). Either *hyaB* or *hydA* was deleted from target strains using a standard protocol for a standard protocol for *S. oneidensis* (Saltikov & Newman, 2003). Deletion strains were initially screened via PCR using gene-specific forward and reverse primers flanking the deletion site and then sequenced (Sanger sequencing, RTSF Genomics Core, Michigan State University) to verify deletion. Bdh-PR plasmids were conjugated into *S. oneidensis* strains using *E. coli* WM3064 using a standard protocol for *S. oneidensis* MR-1 (Coursole & Gralnick, 2010).

Bioelectrochemical system construction and operation

Bioelectrochemical measurements were performed in custom two-chambered bioreactors as previously described (Tefft & TerAvest, 2019). Riboflavin was added to working chamber prior to inoculation to a final concentration of 0.2 μ M using a 0.1mM stock solution. Green LED lights were attached to reactors as previously described (Tefft & TerAvest, 2019). Reactors were connected to a potentiostat (VMP, BioLogic USA) and the working electrode poised at +0.2 V_{Ag/AgCl}. Current was measured every 1 s for the duration of the experiment. Current measurements were collected for at least 16h prior to inoculation. Reactors were inoculated with cultures grown in 50ml of either M5 or M5T medium supplemented with 20mM D, L-lactate. Cultures were grown in 250-ml flasks at 30°C for 17h shaking at 275 rpm. After 17h, 50 μ l 20mM all-*trans*-retinal (vitamin A aldehyde; Sigma-Aldrich, R2500), the essential

TABLE 1 Strains and plasmids used in this study.

Strain or plasmid	Description	Source
<i>E. coli</i>		
WM3064	Conjugation strain for <i>S. oneidensis</i>	Saltikov and Newman (2003)
<i>S. oneidensis</i>		
Δ <i>hyaB</i> Δ <i>hydA</i>	Hydrogenase double knockout mutant	Marshall et al. (2008)
Δ <i>nuoN</i> Δ <i>nqrF1</i>	NADH dehydrogenase double KO strain	Duhl et al. (2018)
Δ <i>nqrF1</i>	Na ⁺ -dependent NADH dehydrogenase KO strain	Duhl et al. (2018)
Δ <i>nuoN</i>	H ⁺ -dependent NADH dehydrogenase KO strain	Duhl et al. (2018)
Δ <i>nuoN</i> Δ <i>nqrF1</i> Δ <i>hyaB</i> Δ <i>hydA</i>	NADH dehydrogenase double KO strain with Hydrogenase knockout	This study
Δ <i>nqrF1</i> Δ <i>hyaB</i> Δ <i>hydA</i>	Na ⁺ -dependent NADH dehydrogenase KO strain with Hydrogenase knockout	This study
Δ <i>nuoN</i> Δ <i>hyaB</i> Δ <i>hydA</i>	H ⁺ -dependent NADH dehydrogenase KO strain with Hydrogenase knockout	This study
Plasmids		
pSMV3.0	R6K origin vector	
pSMV3.0 Δ <i>hyaB</i>	In-frame deletion plasmid for <i>hyaB</i>	This study
pSMV3.0 Δ <i>hydA</i>	In-frame deletion plasmid for <i>hydA</i>	This study
pBBR1-MCS2	Kan resistance, broad host vector	Yazynin et al. (1996)
pBdh-PR	pBBR1MCS2 bearing butanediol dehydrogenase and proteorhodopsin	Tefft and TerAvest (2019)

proteorhodopsin cofactor, (Fuhrman et al., 2008) was added to the flasks to a final concentration of 20 μ M and all flasks were returned to incubator, shaking, for 1 h. Adjustments were made to account for the growth defect in $\Delta nuoN\Delta nqrF1$, preculture growth time was extended to 20 h for this strain (Duhl et al., 2018).

Absorbance at 600 nm was determined for each culture using a biophotometer (Eppendorf, D30) before the volume was transferred to a 50 ml conical tube (VWR, 89039–664) and centrifuged for 5 min at 8000 rpm (Thermo Scientific ST8R; Rotor: 75005709). For M5 cultures 100 ml of culture was pelleted. For M5T cultures, 30 ml of culture was pelleted, except for $\Delta nuoN\Delta nqrF1\DeltahyaB\DeltahydA$ where 100 ml was pelleted to account for the growth defect in this strain. Cells were washed in 50 ml of M5 (100 mM HEPES, no carbon source, no tryptone) the supernatant removed and then resuspended in M5 (100 mM HEPES, no carbon source, no tryptone) to $OD_{600} = 3.6$.

The working chamber of each bioelectrochemical system was inoculated with 9 ml of standardized cell suspension using an 18 g needle (Beckton Dickson, 305196) and 10-ml syringe (Beckton Dickson, 302995). Inoculated reactors were exposed to ambient oxygen for 6 h before N_2 gas, 99.9% (Airgas) was bubbled into the reactors through a 0.2 μ m filter. The rate of flow of nitrogen gas was observed using a bubbler attached to the gas outlet line from the reactors. The rate of gas flow was maintained so there was positive pressure against the water in the bubbler and bubble rate was kept constant between reactors.

Reactors remained at +0.2 V_{Ag/AgCl} for 40 h before the potential was changed to -0.5 V_{Ag/AgCl}. After 2 h, sterile, anoxic acetoin solution was added to a final concentration of 1 mM. A 2-ml sample was taken approximately every 24 h using a 21 g needle (Beckton Dickson, 305167) and 3-ml syringe (Beckton Dickson, 309657). One millilitre was used for determination of OD_{600} . One millilitre was transferred to a micro-centrifuge tube (VWR, 20170–038) and frozen at -20°C until preparation for HPLC analysis. Experiments without a set potential on the working electrode were set up as above excepting that immediately after acetoin injection, the potentiostat was disconnected from the working electrodes. Anoxic sodium fumarate was injected into each reactor to a final concentration of 20 mM at 72 h post acetoin injection.

For CCCP experiments, reactors were prepared as above but 24 h after acetoin injection CCCP was added to a final concentration of 125 μ M from a stock dissolved in 100% ethanol via syringe and needle. For control conditions, an equal volume of 100% ethanol was added without CCCP.

HPLC analysis

HPLC analysis was performed as previously described with the following changes (Tefft & TerAvest, 2019). A

0.5 ml/min flow rate was used for better separation of 2,3 butanediol and acetoin at measured concentrations. 2,3-butanediol standards were prepared at 0.01, 0.025, 0.05, 0.1, 0.5, 1 and 5 mM.

Electrode protein quantification

Immediately upon cessation of each experiment, working electrodes were removed from the working chamber and placed in a 50 ml conical tube. The electrodes were frozen at -20°C until protein extraction. Electrodes were prepared by suspending harvested electrodes in 20 ml 0.2 M NaOH. Samples were heated at 95°C in a drying oven (VWR, 89511–404) for 30 min, inverting every 10 min to mix. After heating, 25 μ l of prepared samples were transferred to a clear 96 well plate (VWR, 10062–900). Standards and reagents were prepared using a Pierce BCA protein assay kit (Thermo Scientific) as per protocol. A working reagent volume of 200 μ l was added to each well and incubated at 37°C for 30 min. Absorbance at 562 nm was measured using a synergy H1M plate reader (BioTek) and exported using Gen5 analysis software (BioTek). Protein concentration was determination using a standard bovine serum albumin (BSA) curve.

Data analysis

Analysis of HPLC, protein concentration, OD and current data was performed using Rstudio using the following packages: ggplot2, reshape2, dplyr and TTR (Ulrich, 2017; Wickham, 2007, 2009; Wickham & Francois, 2015).

RESULTS

To determine the role of NADH dehydrogenases in inward electron transfer in *S. oneidensis* MR-1, we compared a background strain without hydrogenases ($\DeltahyaB\DeltahydA$) to strains lacking the hydrogenases and one or more NADH dehydrogenase. The hydrogenase deletion strain was used as the background to rule out H_2 -mediated electron transfer, as in our previous work (Tefft & TerAvest, 2019). We focused on Nuo and Nqr1 because previous work from our group demonstrated the importance of these two complexes under a range of conditions, including aerobic growth, soluble iron reduction and electrode reduction (Duhl et al., 2018; Madsen & TerAvest, 2019). We have not observed significant phenotypes for Nqr2 or Ndh mutants under any tested condition, therefore, they were not included in this study.

As in our previous work, PR and Bdh were constitutively expressed from a plasmid in all strains to enable

light-driven PMF generation and the use of acetoin reduction as an NADH sink (Figure 1). We then pre-grew all strains under aerobic conditions and inoculated into two-chambered electrochemical cells at an optical density (OD_{600}) of 0.2. Because flavins are essential for effective extracellular electron transfer in *S. oneidensis* MR-1, 0.2 μM riboflavin was added to all bioreactors before inoculation (Kotloski & Gralnick, 2013; Marsili et al., 2008). To facilitate cell attachment to the electrode and oxidation of any stored or carryover organic carbon, the electrochemical cells were passively aerated, and the electrode was poised at an anodic potential of +0.2 $V_{\text{Ag}/\text{AgCl}}$. After 6 h, N_2 sparging was started and all strains generated anodic current during this phase of the experiment, with $\Delta nuoN\Delta nqrF1\Delta hyaB\Delta hydA$ generating a higher peak anodic current than the other strains (Figure 2A). Anodic current generation increases after N_2 sparging because the cells switch from using O_2 to the electrode as the terminal electron acceptor. After an additional 40 h, the electrode was switched to a cathodic potential of $-0.5 V_{\text{Ag}/\text{AgCl}}$ (Figure 2B). After the potential switch, a spike in cathodic current was observed, and current was allowed to stabilize for 2 h before acetoin injection (time = 0). Under these conditions, the cells do not grow and OD_{600} decreases over time due to electrode attachment and possibly cell death (Figure S1). However, the removal of organic carbon and alternative electron acceptors is essential to interpretation of the experiments. The total protein on the electrodes was evaluated at the end of the experiment and was not significantly different among any of the strains (Figure S2).

As in our previous study, we observed that $\Delta hyaB\Delta hydA$ with PR and Bdh generated cathodic

current over the course of 3 days and accumulated 2,3-butanediol, while sterile controls produced background cathodic current of less than $-5 \mu\text{A}$ and no 2,3-butanediol (Figure 2). In general, cathodic current was unchanged in the $\Delta nuoN\Delta hyaB\Delta hydA$ strain but decreased in the $\Delta nqrF1\Delta hyaB\Delta hydA$ and double knockout strains for the first ~ 1.5 days after acetoin injection (Figure 2B). Deletion of *nuoN* did not affect 2,3-butanediol production, while deletion of *nqrF1* caused a 25% decrease compared with the parent strain at day three (two-tailed *t*-test, $p < 0.05$) (Figure 3). Combined deletion of *nuoN* and *nqrF1* completely blocked electrode-driven 2,3-butanediol production, while deletion of *nqrF1* caused a 25% decrease compared with the parent strain at day three (two-tailed *t*-test, $p < 0.05$) (Figure 3). Combined deletion of *nuoN* and *nqrF1* completely blocked electrode-driven 2,3-butanediol production. 2,3-butanediol accumulation was below detectable levels for all strains when the working electrode was not connected to the potentiostat (data not shown).

Because the $\Delta nuoN\Delta nqrF1\Delta hyaB\Delta hydA$ strain generally grows more poorly than $\Delta hyaB\Delta hydA$, we made several comparisons to determine whether the lack of 2,3-butanediol production was due to a general defect in the strain. First, we compared anodic current generated by all strains in the first phase of the experiment, before switching the electrode to a cathodic potential. We observed that $\Delta nuoN\Delta nqrF1\Delta hyaB\Delta hydA$ produced a peak anodic current over 2-fold higher than the other strains and the total charge transfer in the anodic phase of the experiment was 2.8 times higher than the $\Delta hyaB\Delta hydA$ strain (Figure 2A). We also measured total protein in each BES to rule out possible disparity in cell attachment to the electrode. We found no significant differences between strains in measured protein from electrode or media samples (Figure S2).

We also tested the ability of all strains to transfer electrons from a cathode to fumarate. This activity requires

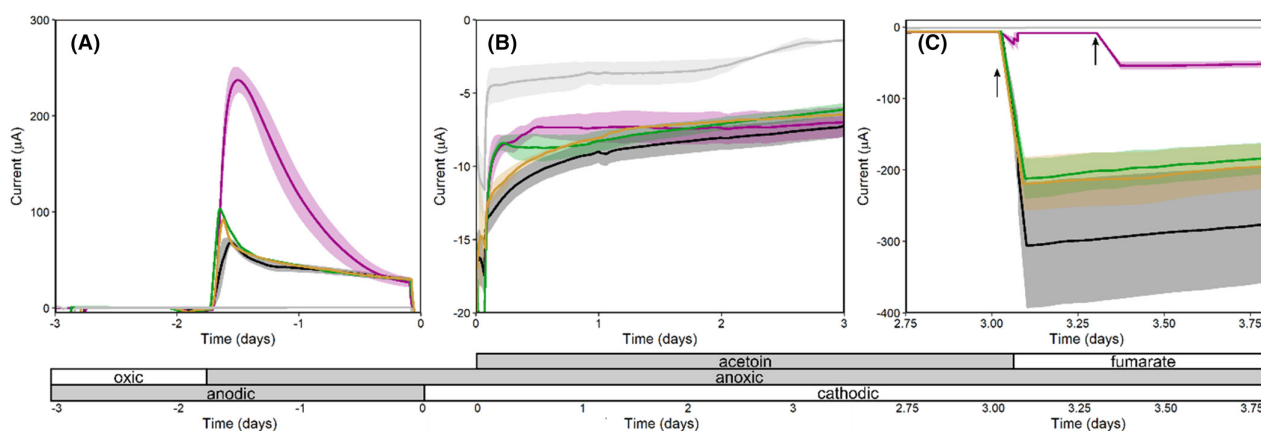


FIGURE 2 Current generation by *S. oneidensis* strains under operation of electrochemical cells. (A) Electrode poised at anodic potential. (B) Electrode poised at cathodic potential. Injection of acetoin to a final concentration of 1 mM occurred at time 0. (C) Black arrows indicate when sodium fumarate was injected to a concentration of 20 mM (second arrow is for $\Delta nuoN\Delta nqrF1\Delta hyaB\Delta hydA$ only). The disparity in time of fumarate injection in $\Delta nuoN\Delta nqrF1\Delta hyaB\Delta hydA$ conditions was due to the fumarate being injected slightly later during the experiment. $\Delta hyaB\Delta hydA$ is shown in black, $\Delta nuoN\Delta hyaB\Delta hydA$ is shown in green, $\Delta nqrF1\Delta hyaB\Delta hydA$ is shown in orange, $\Delta nuoN\Delta nqrF1\Delta hyaB\Delta hydA$ is shown in magenta. Conditions where no cells were added (sterile) are shown in grey. Lines represent the average of three replicates with standard error shown in transparent ribbons. Sterile and $\Delta nqrF1\Delta hyaB\Delta hydA$ conditions are an average of two replicates.

MtrCAB, CymA and FccA, but is not expected to require NADH dehydrogenases (Ross et al., 2011; Rowe et al., 2018, 2021). After 3 days of cathodic operation with acetoin, we injected fumarate to a final concentration of 20 mM and observed an immediate increase in cathodic current (Figure 2C). Strains lacking single NADH dehydrogenases exhibited moderate decreases in fumarate-dependent cathodic current compared with the $\DeltahyaB\DeltahydA$ strain; however, the difference in charge transfer was not significant. The $\Delta nuoN\Delta nqrF1\DeltahyaB\DeltahydA$ strain generated over 3-fold less fumarate-dependent cathodic current. However, all strains exhibited fumarate-dependent current >5-fold higher than acetoin-dependent current.

We evaluated the ability of the $\Delta nuoN\Delta nqrF1\DeltahyaB\DeltahydA$ strain to reduce acetoin to 2,3-butanediol

under conditions where it grows well, that is, in oxic lysogeny broth (LB). Cells were grown in flasks to ensure oxygen availability and sampled periodically to measure growth and 2,3-butanediol. We observed that both the control and NADH dehydrogenase double mutant strain produced ~1 mM 2,3-butanediol from 10 mM acetoin under this condition (Figure 4A). In this condition, the NADH dehydrogenase mutant strain produced slightly higher levels of 2,3-butanediol, possibly due to a build-up of NADH in the cytoplasm, as previously observed (Duhl & Ter Avest, 2019). The 2,3-butanediol concentration decreased during stationary phase for both strains, possibly due to back conversion to acetoin after major electron donors in the medium were consumed.

We hypothesized that a source of PMF would be essential for inward electron transfer to acetoin if the Nuo and Nqr1 were functioning in reverse to generate NADH. The experimental conditions used for inward electron transfer do not provide a known route for PMF generation by any native process, that is, there is no source of ATP that could be hydrolysed by the F_0F_1 ATP synthase and no electron acceptor energetically 'downhill' of menaquinone (such as fumarate or oxygen) that could be used for forward reactions of the electron transport chain. We previously observed that the presence of functional PR and green light enhanced inward electron transfer, supporting the hypothesis that PMF is important for electron transfer from a cathode to acetoin (Tefft & TerAvest, 2019).

Here, we tested whether PMF is required for inward electron transfer by adding the protonophore uncoupler carbonyl cyanide m-chlorophenyl hydrazone (CCCP) in experiments with the $\DeltahyaB\DeltahydA$ strain (all NADH dehydrogenases present). In these experiments, CCCP dissolved in ethanol was injected into the bioelectrochemical systems to a final concentration of 125 μ M approximately 24 h after acetoin injection (Figure 5). CCCP has poor solubility in water which necessitated

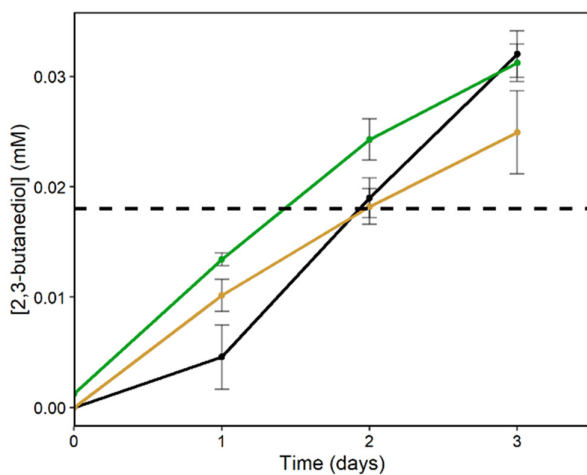


FIGURE 3 2,3-butanediol accumulation. $\DeltahyaB\DeltahydA$ is shown in black, $\Delta nuoN\DeltahyaB\DeltahydA$ is shown in green, $\Delta nqrF1\DeltahyaB\DeltahydA$ is shown in orange. Reactors with an unpoised electrode and $\Delta nuoN\Delta nqrF1\DeltahyaB\DeltahydA$ had 2,3-butanediol values that fell below the limit of detection shown in the dotted black line. Lines represent the average of three replicates with standard error shown in transparent ribbons.

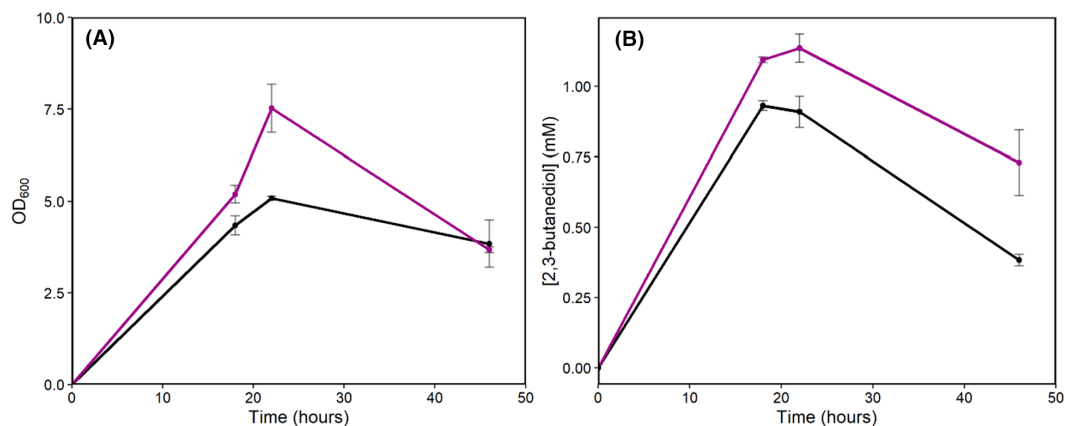


FIGURE 4 (A) Cell density and (B) 2,3-butanediol accumulation of *S. oneidensis* strains grown in LB with shaking in 250-ml flasks. $\DeltahyaB\DeltahydA$ is shown in black, $\Delta nuoN\Delta nqrF1\DeltahyaB\DeltahydA$ is shown in magenta. Each point represents the average of three replicates for $\Delta nuoN\Delta nqrF1\DeltahyaB\DeltahydA$ and two replicates for $\DeltahyaB\DeltahydA$ with standard error or range, respectively, shown in error bars.

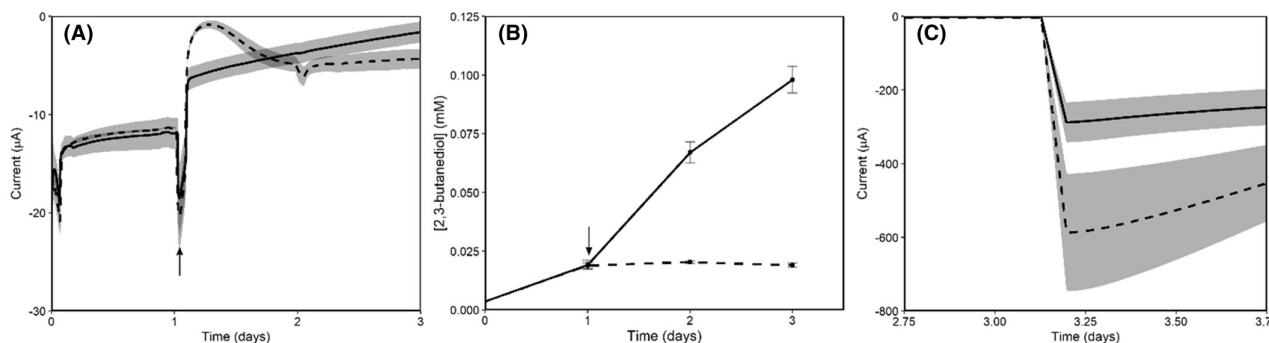


FIGURE 5 (A) Cathodic current in electrochemical cells with modified *S. oneidensis*. (B) 2,3-butanediol accumulation in the same experiment. (C) Cathodic current after addition of 20 mM fumarate. Black arrows indicate when CCCP was injected to a concentration of 125 μM . Dotted lines indicate reactors with CCCP injection and solid lines represent reactors with ethanol only injection. Each point represents the average of three replicates with standard error shown in error bars or transparent ribbons.

the use of ethanol as a carrier to achieve target concentrations. Upon CCCP injection, cathodic current decreased and 2,3-butanediol accumulation slowed (Figure 5B). In systems with ethanol injection alone as a negative control, 2,3-butanediol concentration continued to increase for another 2 days, at a faster rate than in systems without ethanol or CCCP injection (Figure 2). To test whether the effect of CCCP was caused specifically by the loss of PMF or simply by cell death and lysis caused by CCCP, we injected fumarate into the electrochemical cells on day 3 as described above. We observed that fumarate-dependent cathodic current increased similarly in both conditions (Figure 5C).

DISCUSSION

Our previous work provided proof of the concept that the extracellular electron transfer pathway of *S. oneidensis* can be driven in reverse to power NADH-dependent reactions in the cytoplasm. Here, we showed that deletion of the two key NADH dehydrogenases, Nuo and Nqr1, prevented accumulation of 2,3-butanediol to detectable levels, indicating that these complexes are critical to inward electron transfer from the electrode. We observed that deletion of either NADH dehydrogenase alone had little to no effect, consistent with our previous observations that Nuo and Nqr1 have overlapping functions but one or the other is required for aerobic growth or current generation at an anode (Duhl et al., 2018; Madsen & TerAvest, 2019).

Although the $\Delta\text{nnoN}\Delta\text{nqrF1}$ NADH dehydrogenase deletion strain has a growth defect compared with the parent strain, the lack of acetoin reduction cannot be attributed to this general defect. The $\Delta\text{nnoN}\Delta\text{nqrF1}$ NADH dehydrogenase mutant was capable of acetoin reduction in oxic-rich medium (Figure 5) and had cell mass on the electrode consistent with other strains (Figure S2). Further, the double NADH dehydrogenase deletion strain produced a higher peak anodic current

than any other strain (Figure 2A). We speculate that this was due to a greater amount of stored organic carbon accumulated in the cells during aerobic growth in flasks. The $\Delta\text{nnoN}\Delta\text{nqrF1}$ NADH dehydrogenase mutant has a reduced respiration rate which reduces its ability to oxidize residual organic carbon during the aerobic phases of the experiment (Duhl & Ter Avest, 2019). It is not likely that cell death was responsible for the lack of acetoin reduction as the strain was capable of elevated electron transfer to fumarate (Figure 2C), albeit at a reduced rate compared to the hydrogenase mutant. These results point to a role of the NADH dehydrogenases specifically in electron transfer from a cathode to acetoin.

While the NADH dehydrogenases had a major impact on 2,3-butanediol production, anodic current and fumarate-dependent current, the changes in cathodic current were smaller. This is due in part to abiotic processes occurring at the cathode, which account for $\sim 5 \mu\text{A}$. We also observed biotic current that was not associated with 2,3-butanediol production in $\Delta\text{nnoN}\Delta\text{nqrF1}$. At this time, it remains unclear what other biotic process is occurring, although one possibility is reduction of trace oxygen in the system.

We also found that the electron transfer rate to acetoin is orders of magnitude lower than the rate for outward electron transfer to an anode or inward electron transfer to a native terminal electron acceptor, such as fumarate or oxygen (Ringeisen et al., 2006; Ross et al., 2011; Rowe et al., 2018, 2021). This observation provides evidence that the Mtr pathway is not the rate-limiting step for electrode-driven acetoin reduction because electron transfer to fumarate occurred at a much faster rate than electron transfer to acetoin although both are dependent on the Mtr pathway (Figure 1). Thermodynamic analysis suggests that electron transfer from menaquinol to NAD^+ could be the rate-limiting step, considering that this reaction is highly unfavorable with $\Delta_r G^{\text{m}} = +46.2 \text{ kJ/mol}$ (Flamholz et al., 2012). We hypothesize that electron transfer from menaquinol

to NAD⁺ can only occur at a significant rate by coupling it to the thermodynamically favourable movement of protons from the periplasm to the cytoplasm via electrogenic NADH dehydrogenases. Favourable proton movement down the gradient is coupled with many otherwise unfavourable but necessary cellular processes, including ATP synthesis, flagellar rotation and transport of solutes against their gradients. There are also confirmed examples of SMF dissipation driving unfavourable redox reactions, such as electron transfer from NADH to ferredoxin catalysed by the Rnf complex (Westphal et al., 2018). Our results with NADH deletion strains support the hypothesis that PMF is needed to drive reverse electron transfer; when the two key electrogenic NADH dehydrogenases were deleted, electrode-driven reduction was dramatically inhibited, although Ndh (the uncoupling NADH dehydrogenase) was still present.

The hypothesis that PMF drives inward electron transport is further supported by results with CCCP injection, which showed that when the uncoupler is added, electrode-driven acetoin reduction is greatly reduced. CCCP increases membrane permeability to protons and inhibits cells from maintaining PMF, therefore, it blocks processes that require PMF, such as ATP synthesis. Fumarate injection after CCCP injection indicated that the uncoupler did not inhibit electron transfer to an energetically downhill electron acceptor, suggesting that the cessation of 2,3-butanediol production was not due to a general effect of CCCP, such as toxicity. Surprisingly, an increase in 2,3-butanediol production (relative to experiments shown in Figure 2) was observed with ethanol alone and was not accompanied by an increase in current (Figure 5). We speculate that *S. oneidensis* oxidized the ethanol to gain NADH that was used to reduce acetoin. We also observed that cathodic current recovered somewhat after ~1 day in the bioreactors with CCCP, although no further 2,3-butanediol was accumulated. Previous reports indicate that CCCP can be degraded by light (Pistorius et al., 1975). It is not clear why cathodic current would recover but not 2,3-butanediol production. We speculate that regulatory changes caused by the CCCP may have activated an alternate electron transfer pathway, although the identity of the terminal electron acceptor remains unknown. In future work, we will investigate alternate methods for dissipating PMF that do not involve introduction of CCCP or an organic carbon source.

AUTHOR CONTRIBUTIONS

Nicholas M Tefft: Formal analysis (equal); investigation (lead); methodology (equal); visualization (lead); writing – original draft (lead); writing – review and editing (equal). **Kathryne C Ford:** Formal analysis (supporting); investigation (supporting); methodology (supporting); visualization (supporting); writing – review and editing (supporting). **Michaela TerAvest:**

Formal analysis (equal); funding acquisition (lead); investigation (supporting); methodology (equal); project administration (lead); visualization (supporting); writing – original draft (supporting); writing – review and editing (equal).

ACKNOWLEDGMENTS

This material is based upon work supported by the National Science Foundation Graduate Research Fellowship under Grant No. (DGE-1848739) to Kathryne C. Ford, and a National Science Foundation CAREER Award (1750785) and 2018 Beckman Young Investigator Award to Dr. Michaela TerAvest.

FUNDING INFORMATION

This material is based upon work supported by the National Science Foundation Graduate Research Fellowship under Grant No. (DGE-1848739) to Kathryne C. Ford, and a National Science Foundation CAREER Award (1750785) and 2018 Beckman Young Investigator Award to Dr. Michaela TerAvest.


CONFLICT OF INTEREST

The authors declare no conflict of interest.

DATA AVAILABILITY STATEMENT

All data are available upon request.

ORCID

Michaela A. TerAvest  <https://orcid.org/0000-0002-5435-3587>

REFERENCES

- Bond, D. & Lovley, D. (2003) Electricity production by *Geobacter sulfurreducens* attached to electrodes. *Applied and Environmental Microbiology*, 69, 1548–1555.
- Bose, A., Gardel, E.J., Vidoudez, C., Parra, E.A. & Girguis, P.R. (2014) Electron uptake by iron-oxidizing phototrophic bacteria. *Nature Communications*, 5, 3391.
- Coursolle, D. & Gralnick, J.A. (2010) Modularity of the Mtr respiratory pathway of *Shewanella oneidensis* strain MR-1. *Molecular Microbiology*, 77, 995–1008.
- Duhl, K.L., Tefft, N.M. & Ter Avest, M.A. (2018) *Shewanella oneidensis* MR-1 utilizes both sodium- and proton-pumping NADH dehydrogenases during aerobic growth. *Applied and Environmental Microbiology*, 84, e00415-18.
- Duhl, K.L. & Ter Avest, M.A. (2019) *Shewanella oneidensis* NADH dehydrogenase mutants exhibit an amino acid synthesis defect. *Frontiers in Energy Research*, 7, 116.
- Eddie, B.J., Wang, Z., Herve, W.J., Leary, D.H., Malanoski, A.P., Tender, L.M. et al. (2017) Metatranscriptomics supports the mechanism for biocathode electroautotrophy by *Candidatus Tenderia electrophaga*. *mSystems*, 2, e00002-17.
- Flamholz, A., Noor, E., Bar-Even, A. & Milo, R. (2012) eQuilibrator—the biochemical thermodynamics calculator. *Nucleic Acids Research*, 40, D770–D775.
- Fuhrman, J.A., Schwalbach, M.S. & Stingl, U. (2008) Proteorhodopsins: an array of physiological roles? *Nature Reviews. Microbiology*, 6, 488–494.
- Hernandez, M.E. & Newman, D.K. (2001) Extracellular electron transfer. *Cellular and Molecular Life Sciences*, 58, 1562–1571.

- Kotloski, N.J. & Gralnick, J.A. (2013) Flavin electron shuttles dominate extracellular electron transfer by *Shewanella oneidensis*. *mBio*, 4, e00553-12.
- Levar, C.E., Chan, C.H., Mehta-Kolte, M.G. & Bond, D.R. (2014) An inner membrane cytochrome required only for reduction of high redox potential extracellular electron acceptors. *mBio*, 5, e02034.
- Madsen, C.S. & TerAvest, M.A. (2019) NADH dehydrogenases Nuo and Nqr1 contribute to extracellular electron transfer by *Shewanella oneidensis* MR-1 in bioelectrochemical systems. *Scientific Reports*, 9, 14959.
- Marritt, S.J., Lowe, T.G., Bye, J., McMillan, D.G.G., Shi, L., Fredrickson, J. et al. (2012) A functional description of CymA, an electron-transfer hub supporting anaerobic respiratory flexibility in *Shewanella*. *The Biochemical Journal*, 444, 465 LP – 474.
- Marshall, M.J., Plymale, A.E., Kennedy, D.W., Shi, L., Wang, Z., Reed, S.B. et al. (2008) Hydrogenase- and outer membrane c-type cytochrome-facilitated reduction of technetium(VII) by *Shewanella oneidensis* MR-1. *Environmental Microbiology*, 10, 125–136.
- Marsili, E., Baron, D.B., Shikhare, I.D., Coursolle, D., Gralnick, J.A. & Bond, D.R. (2008) *Shewanella* secretes flavins that mediate extracellular electron transfer. *Proceedings of the National Academy of Sciences*, 105, 3968–3973.
- McMillan, D.G.G., Marritt, S.J., Butt, J.N. & Jeuken, L.J.C. (2012) Menaquinone-7 is specific cofactor in tetraheme quinol dehydrogenase CymA. *The Journal of Biological Chemistry*, 287, 14215–14225.
- Myers, C.R. & Neelson, K.H. (1988) Bacterial manganese reduction and growth with manganese oxide as the sole electron acceptor. *Science (80-)*, 240, 1319–1321.
- Nevin, K.P., Hensley, S.A., Franks, A.E., Summers, Z.M., Ou, J., Woodard, T.L. et al. (2011) Electrosynthesis of organic compounds from carbon dioxide is catalyzed by a diversity of acetogenic microorganisms. *Applied and Environmental Microbiology*, 77, 2882–2886.
- Pappijn, C.A.R., Ruitenbeek, M., Reyniers, M.-F. & Van Geem, K.M. (2020) Challenges and opportunities of carbon capture and utilization: electrochemical conversion of CO₂ to ethylene. *Frontiers in Energy Research*, 8, 557466.
- Pistorius, E.K., Gewitz, H.-S., Voss, H. & Vennesland, B. (1975) Cyanide generation from carbonylcyanide m-chlorophenylhydrazone and illuminated grana or algae. *FEBS Letters*, 59, 162–166.
- Rabaey, K. & Rozendal, R.A. (2010) Microbial electrosynthesis – revisiting the electrical route for microbial production. *Nature Reviews. Microbiology*, 8, 706–716.
- Richardson, D.J., Butt, J.N., Fredrickson, J.K., Zachara, J.M., Shi, L., Edwards, M.J. et al. (2012) The ‘porin–cytochrome’ model for microbe-to-mineral electron transfer. *Molecular Microbiology*, 85, 201–212.
- Ringeisen, B.R., Henderson, E., Wu, P.K., Pietron, J., Ray, R., Little, B. et al. (2006) High power density from a miniature microbial fuel cell using *Shewanella oneidensis* DSP10. *Environmental Science & Technology*, 40, 2629–2634.
- Ross, D.E., Flynn, J.M., Baron, D.B., Gralnick, J.A. & Bond, D.R. (2011) Towards electrosynthesis in *Shewanella*: energetics of reversing the Mtr pathway for reductive metabolism. *PLoS One*, 6, e16649.
- Rowe, A.R., Chellamuthu, P., Lam, B., Okamoto, A. & Neelson, K. (2015) Marine sediments microbes capable of electrode oxidation as a surrogate for lithotrophic insoluble substrate metabolism. *Frontiers in Microbiology*, 5, 784.
- Rowe, A.R., Rajeev, P., Jain, A., Pirkadian, S., Okamoto, A., Gralnick, J.A. et al. (2018) Tracking electron uptake from a cathode into *Shewanella* cells: implications for energy acquisition from solid-substrate electron donors. *mBio*, 9, e02203-17.
- Rowe, A.R., Salimijazi, F., Trutschel, L., Sackett, J., Adesina, O., Anzai, I. et al. (2021) Identification of a pathway for electron uptake in *Shewanella oneidensis*. *Communications Biology*, 4, 1–10.
- Saltikov, C.W. & Newman, D.K. (2003) Genetic identification of a respiratory arsenate reductase. *Proceedings of the National Academy of Sciences of the United States of America*, 100, 10983–10988.
- Shi, L., Fredrickson, J.K. & Zachara, J.M. (2014) Genomic analyses of bacterial porin–cytochrome gene clusters. *Frontiers in Microbiology*, 5, 657.
- Shi, L., Rosso, K.M., Clarke, T.A., Richardson, D.J., Zachara, J.M. & Fredrickson, J.K. (2012) Molecular underpinnings of Fe(III) oxide reduction by *Shewanella oneidensis* MR-1. *Frontiers in Microbiology*, 3, 50.
- Spero, M.A., Aylward, F.O., Currie, C.R. & Donohue, T.J. (2015) Phylogenomic analysis and predicted physiological role of the proton-translocating NADH:quinone oxidoreductase (complex I) across bacteria. *mBio*, 6, e00389-15.
- Tefft, N.M. & TerAvest, M.A. (2019) Reversing an extracellular electron transfer pathway for electrode-driven acetoin reduction. *ACS Synthetic Biology*, 8, 1590–1600.
- Ulrich, J. (2017) *TTR: technical trading rules*. R Packag version 023-2.
- Westphal, L., Wiechmann, A., Baker, J., Minton, N.P. & Müller, V. (2018) The Rnf complex is an energy-coupled transhydrogenase essential to reversibly link cellular NADH and ferredoxin pools in the acetogen *Acetobacterium woodii*. *Journal of Bacteriology*, 200, e00357-18.
- Wickham, H. (2007) Reshaping data with the reshape package. *Journal of Statistical Software*, 21, 1–20.
- Wickham, H. (2009) *ggplot2 elegant graphics for data analysis*.
- Wickham, H. & Francois, R. (2015) *Dplyr: a grammar of data manipulation*. R Packag version 042.3.
- Yazynin, S.A., Deyev, S.M., Jucović, M. & Hartley, R.W. (1996) A plasmid vector with positive selection and directional cloning based on a conditionally lethal gene. *Gene*, 169, 131–132.

SUPPORTING INFORMATION

Additional supporting information can be found online in the Supporting Information section at the end of this article.

How to cite this article: Tefft, N.M., Ford, K. & TerAvest, M.A. (2023) NADH dehydrogenases drive inward electron transfer in *Shewanella oneidensis* MR-1. *Microbial Biotechnology*, 16, 560–568. Available from: <https://doi.org/10.1111/1751-7915.14175>